Journal of Molecular Catalysis A: Chemical 336 (2011) 34–41

Contents lists available at ScienceDirect

Journal of Molecular Catalysis A: Chemical

journal homepage: www.elsevier.com/locate/molcata

Influences of alkaline treatment on the structure and catalytic performances of ZSM-5/ZSM-11 zeolites with alumina as binder

Xiujie Li, Chuanfu Wang, Shenglin Liu, Wenjie Xin, Yuzhong Wang, Sujuan Xie, Longya Xu*

State Key Laboratory of Catalysis, Dalian Institute of Chemical Physics, Chinese Academy of Sciences, 457 Zhongshan Road, Dalian 116023, China

ARTICLE INFO

Article history:
Received 15 July 2010
Received in revised form
23 November 2010
Accepted 12 December 2010
Available online 8 January 2011

Keywords:
Alkaline treatment
Alumina binder
ZSM-5/ZSM-11
1-Hexene aromatization

ABSTRACT

Influences of alkaline treatment on the structural properties and catalytic performances of ZSM-5/ZSM-11 composite zeolites with alumina as binder at different preparation steps were studied in the present investigation. Temperature-programmed desorption of ammonium (NH_3-TPD) and pyridine infrared (Py-IR) spectra revealed that alkaline treatment sequences changed both the distribution and amount of the acidities in the ZSM-5/ZSM-11-Al_2O_3 samples. The mesopores created by alkaline treatment were found beneficial for the diffusion of aromatic molecules, as determined by the xylene-uptake experiments using a tapered element oscillating microbalance (TEOM). In 1-hexene isomerization and aromatization reactions, the sample after extrusion followed by alkaline treatment exhibited excellent aromatization activity and stability compared with other samples undergoing different treatment sequences. The enhanced catalytic performance could be attributed to the redistribution of acid sites and introduction of more mesopores.

1. Introduction

Creation of mesopores in micropore zeolite particle to increase the accessibility of reactant molecules to internal surface has gradually become an interesting topic in recent years [1–5]. A variety of methods have been reported for the introduction of mesopores in micropore materials among which alkaline treatment attracts more attention due to its simplicity and reproducibility [6–11]. Thus far, most of the research focused on MFI zeolite, especially on ZSM-5 for its promising fuel upgrading performances [9,12–16]. After alkaline treatment, ZSM-5 zeolite showed higher catalytic activity and better stability in olefin to aromatics reactions as a result of the enhanced acid site accessibility in hierarchical porous structure [14–16]. The aluminum atom in ZSM-5 framework proved to be important in controlling the silicon extraction process. Meanwhile, Si/Al ratio was also a key factor for the introduction of mesopore without affecting micropore structure and acidity [1,17,18]. The optimal framework Si/Al molar ratio for desilication was found to range from 25 to 50 [17,18]. However, whether the extra-framework aluminum species [19], especially the existence of alumina binder, will affect the de-silicon process is still unknown.

In order to improve the mechanical strength of zeolite for industrial applications, addition of binder is necessary during the catalyst preparation process [20]. Usually, binders like SiO_2 or Al_2O_3 are considered catalytically inert for the reaction. However, during the alkaline treatment process, alkaline solution may interact with both binder and zeolites. And enhanced hardness was observed on extrudates after alkaline treatment as reported by Groen et al. [21]. As far as the catalytic performance is concerned, few reports could be found about the optimal alkali-treatment condition for bindered zeolite samples. The best preparation sequence for catalysts, *e.g.*, before or after extruder and containing templates or not, is very important for their industrial application. So far, little information is available in the literature due to technical arts or trade secrets. Here, more efforts were put on selecting an optimal treatment condition for zeolite sample with the existence of binder.

In this contribution, influences of alkaline treatment sequence on structure and the ensuing catalytic performance of catalyst in an olefin aromatization reaction were studied. ZSM-5/ZSM-11 composite zeolite was chosen as a model catalyst since it had been successfully industrialized in alkylation reaction of benzene with the dilute ethylene in FCC off-gas [22,23]. And it also showed good catalytic performances in the 1-hexene aromatization reaction [24]. Alumina was selected as binder with a weight percent of 20%. Four catalysts with different alkaline treatment sequences were prepared and evaluated over 1-hexene isomerization and aromatization reaction. NH_3-TPD and Py-IR spectra were applied to detect the acidity information before and after alkaline treatments. Pore structure information and the mass transfer factors were further characterized by N_2 adsorption and *m*-xylene adsorption

* Corresponding author. Tel.: +86 411 8437 9279; fax: +86 411 8469 3292.
E-mail addresses: lyxu@dicp.ac.cn, xiujieli@dicp.ac.cn (L. Xu).

1381-1169/$ – see front matter © 2011 Elsevier B.V. All rights reserved.
doi:10.1016/j.molcata.2010.12.007

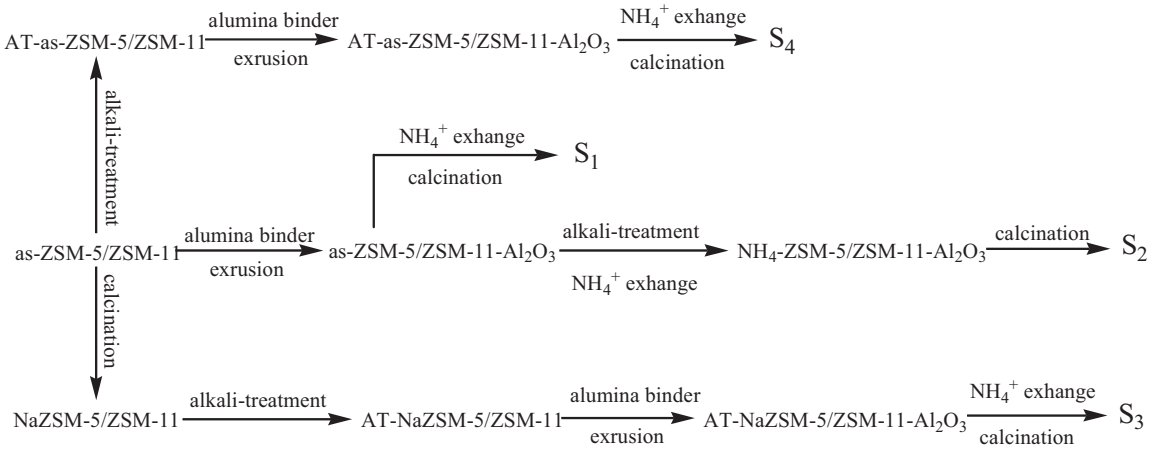

Scheme 1. Preparation methods of ZSM-5/ZSM-11-Al_2O_3 samples with different alkaline treatment conditions.

experiments using tapered element oscillating microbalance (TEOM).

2. Experimental

2.1. Catalyst preparation and evaluation

NaZSM-5/ZSM-11 composite zeolite (Si/Al molar ratio = 25) was obtained from Fushun Petrochemical Corporation of SINOPEC, China. Detailed synthesis conditions were described in Ref. [25]. Sample 1 was prepared by extruding a mixture of alumina and Na-ZSM-5/ZSM-11 zeolite into strips of 2 mm diameter. Sample 2 was obtained by leaching Sample 1 with 0.2 M NaOH solution at 80 °C for 2 h (solution/zeolite ratio of 5 cm^3/g). Samples 3 and 4 were NaZSM-5/ZSM-11 zeolite without and with organic template, subjected to alkaline treatment and extrusion process, respectively. All the samples in this study were exchanged with 0.5 M NH_4NO_3 solution at 80 °C for 2 h and then calcined at 520 °C to make the zeolite to transform from Na-form to H-form. Detailed preparation method was described in Scheme 1. Four samples of the above in H-form were defined as S_1, S_2, S_3 and S_4, respectively.

The 1-hexene aromatization and isomerization reaction was performed in a continuous flow reactor. Typically, 3.5 g catalyst was loaded in the middle part of fixed-bed stainless reactor with 320 mm in length and 12 mm in diameter. The reaction was performed at 350 °C, 0.5 MPa with a weight hourly space velocity (WHSV) of 2 h^{-1}. Before the reaction, the catalyst was pretreated at 500 °C for 2 h in nitrogen flow to remove the water. Hexene feed (97% 1-hexene, 3% 2-hexene) was introduced to the reactor when the temperature decreased to 350 °C. The gas and liquid products were analyzed by a Varian-3800 gas chromatograph equipped with an FID detector and a 100 m PONA capillary column.

2.2. Cyclo-hexane and m-xylene uptake measurements

A Rupprecht and Patashnick TEOM-1500 mass analyzer was used to measure the uptakes of *cyclo*-hexane and *m*-xylene in the calcined and alkaline-treated samples. 50 mg zeolite samples were loaded in the TEOM. Prior to the uptake experiments, the samples were heated in 20 ml/min Ar flow at a rate of 5 °C/min to 500 °C for 240 min and then cooled to 120 °C or 150 °C. As the baseline was stable, adsorption of *cyclo*-hexane or *m*-xylene in flowing Ar (total flow rate of 20 ml/min) was subsequently measured at 120 and 150 °C, respectively. The corresponding mass changes information during the uptake process was recorded upon time.

2.3. Characterization

2.3.1. XRD and SEM measurements

X-ray diffraction (XRD) patterns were obtained at room temperature on a Rigaku D/Max-RB diffractometer using Cu-Kα radiation. Powder diffractograms of samples were recorded over a range of 2θ values from 5° to 50° under the conditions of 40 kV and 100 mA at a scanning rate of 5°/min. Scanning electron micrographs (SEM) were taken using a Quanta 200F field-emission microscope.

2.3.2. NH_3-TPD measurements

Temperature-programmed desorption of ammonium (NH_3-TPD) measurements were carried out in a conventional U-shaped stainless-steel micro-reactor (*i.d.* = 4 mm) using flowing helium (He) as the carrier gas. The NH_3 concentration in the NH_3-TPD process was monitored by an on line gas chromatograph (Shimadzu GC-8A) equipped with a TCD detector. Typically, 140 mg sample was pretreated at 600 °C for 1 h in the flow of He (25 ml/min), cooled to 150 °C and saturated with NH_3 gas. Then, the sample was purged with pure He stream for certain time until a stable baseline was obtained. Subsequently NH_3-TPD experiment was carried out in the range of 150–600 °C at a heating rate of 18.8 °C/min.

2.3.3. FT-IR spectra

FT-IR spectra were recorded using Bruker Vertex 70 infrared spectrometer in the range of 400–4000 cm^{-1} with a resolution of 4 cm^{-1} on thin wafers of samples. Prior to pyridine sorption the wafers were degassed under vacuum at 500 °C (*ca.*10^{-2} Torr) for 1 h. Then the samples were cooled to room temperature and IR spectra were recorded as the background. Adsorption of pyridine vapor was achieved at room temperature for 30 min. After subsequent evacuation at 150 °C for 0.5 h, IR-pyridine spectra were recorded. The ratio of Brønsted to Lewis acids was obtained by using corrections developed by Emeis for porous aluminosilicates [26].

2.3.4. N_2 adsorption measurements

Nitrogen adsorption experiments were performed at −196 °C on an ASAP-2000 system in the static measurement mode. Samples were outgassed at 350 °C for 10 h before the measurements. Specific surface areas were calculated by the BET method, the pore volume was determined by N_2 adsorption at a relative pressure of 0.98.

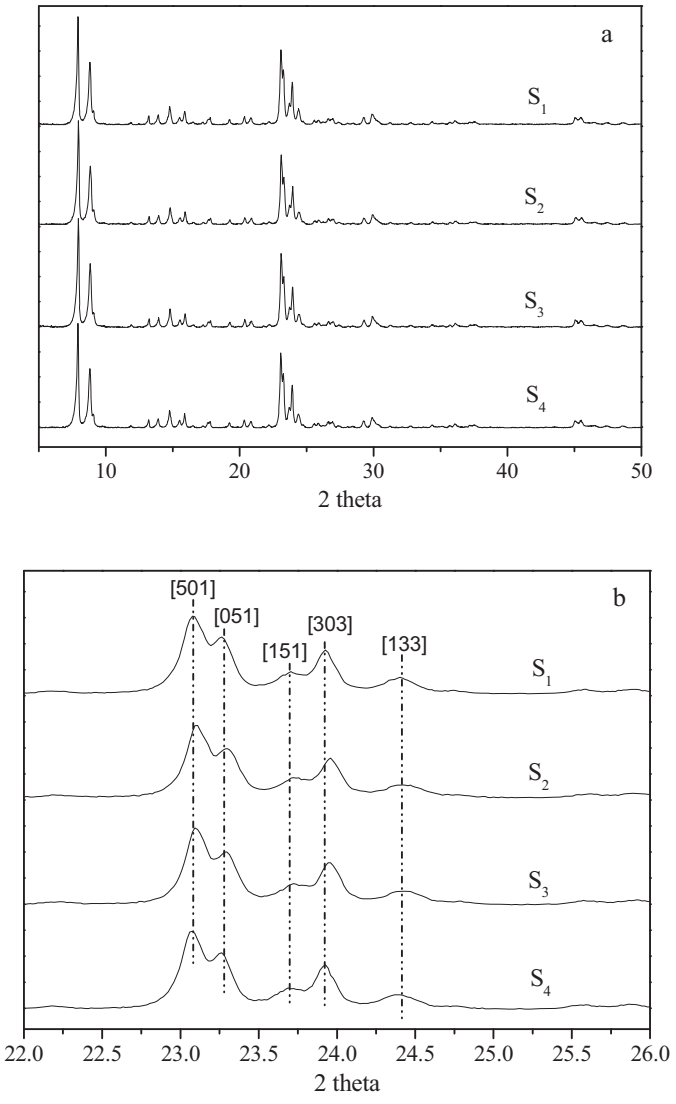

Fig. 1. XRD patterns of HZSM-5/ZSM-11-Al_2O_3 samples with different alkaline treatment conditions: (a) 5–50° and (b) 22–26°.

3. Results and discussions

3.1. Structure and morphology of ZSM-5/ZSM-11-Al_2O_3 samples under different alkali-treatment conditions

Fig. 1a shows the XRD patterns of untreated ZSM-5/ZSM-11-Al_2O_3 and samples with different alkaline treatment processes. S_1 exhibited the typical diffraction peaks of ZSM-5/ZSM-11 zeolite locating at 7.9°, 8.8°, 23.2° and 23.9°, respectively [27]. To give clearer diffraction peaks information about ZSM-5/ZSM-11, the 2θ diffraction angles between 22.0° and 26.0° were magnified in Fig. 1b with corresponding $h\,k\,l$ faces labeled. No preferential losses of peak intensity could be observed on the samples after different alkaline treatment sequence, which confirmed the intact zeolite crystalline structure in all samples irrespective of the treatment conditions. Besides, the diffraction peak assigned to γ-Al_2O_3 could not be observed in the XRD patterns which may be due to the low alumina content in the sample.

In order to get more information about the sample morphology before and after alkaline treatments, SEM images were taken and shown in Fig. 2. It could be seen that ZSM-5/ZSM-11 zeolite particles agglomerated and the particle size was around 2 μm. Alumina existed in disordered and irregular state. As compared to HZSM-5/HZSM-11, S_1, S_2, S_3 and S_4 exhibited irregular shapes due to the existence of alumina binder. No obvious changes were found upon the alkaline treatment, since S_1 showed similar shape to S_2, S_3 and S_4. Besides, alkaline treatment did not show too much influence on the particle. Grooves and defects could not be observed obviously on the zeolite surface as reported by other researchers [9,16].

3.2. Acidity of ZSM-5/ZSM-11-Al_2O_3 samples under different alkali-treatment conditions

3.2.1. NH_3-TPD profiles

Alkaline treatment may lead to the extraction of framework silicon in zeolite and the corresponding acidity changes. Acidity amount and strength variations of the samples were characterized by NH_3-TPD measurements. As shown in Fig. 3, two main desorption peaks could be differentiated on S_1 sample locating at 227 and 415 °C, respectively (defined as *l* and *h*), which was attributed to the desorption of NH_3 molecules from weak and strong acid sites. A shoulder peak at 275 °C could be observed and defined as *m*. Compared with the NH_3-TPD profiles of ZSM-5/ZSM-11 and Al_2O_3 shown in Fig. S1, it could be deduced that the desorption peak at higher temperature (*h*) mainly came from the ZSM-5/ZSM-11 zeolite. And the *l* and *m* peak contained the contribution of both ZSM-5/ZSM-11 zeolite and alumina binder. After alkaline treatment the *h* desorption peak of S_2, S_3 and S_4 shifted to lower temperature, which suggested the weakening of the strong acid sites for alkaline solution leaching samples.

S_2 was derived from the NaOH leaching of S_1, its total line intensity became weaker than that of S_1. However, the peak intensity at 275 °C increased at the loss of peak *l* and *h* indicating that alkaline treatment changed the acidity distribution. In order to give quantitative information about the acidity changes, deconverlutions of different profiles were made and the results were listed in Table 1. Alkaline treatment after extrusion led to the loss of the partial acid sites. The total acidity density decreased from 562 μmol/g in S_1 to 523 μmol/g in S_2. The number of medium acid sites increased at the loss of strong acid sites at high temperature. Such acidity changes were different from the previous observation of Groen et al. [17,18]. To verify the essence of acidity changes, NH_3-TPD profiles of ZSM-5/ZSM-11 before and after alkaline treatment were measured and shown in Fig. S1. Its changes followed the same trend as previous report. Thus, the introduction of alumina binder led to the different acidity changes in S_2. The state and textual properties

Table 1
Acidity distribution of the samples with different alkali-treatment conditions.

Sample	*l* (μmol/g)[a]	*m* (μmol/g)[a]	*h* (μmol/g)[a]	Total acid sites (μmol/g)[a]	B/L (150 °C desorption)[b]	B/L (300 °C desorption)[b]
S_1	90	92	380	562	0.91	2.26
S_2	77	101	345	523	2.25	3.83
S_3	89	123	397	609	2.00	3.00
S_4	95	145	398	638	1.92	2.89

[a] Determined by NH_3-TPD profiles.
[b] Determined by Py-IR spectra with different desorption temperatures.

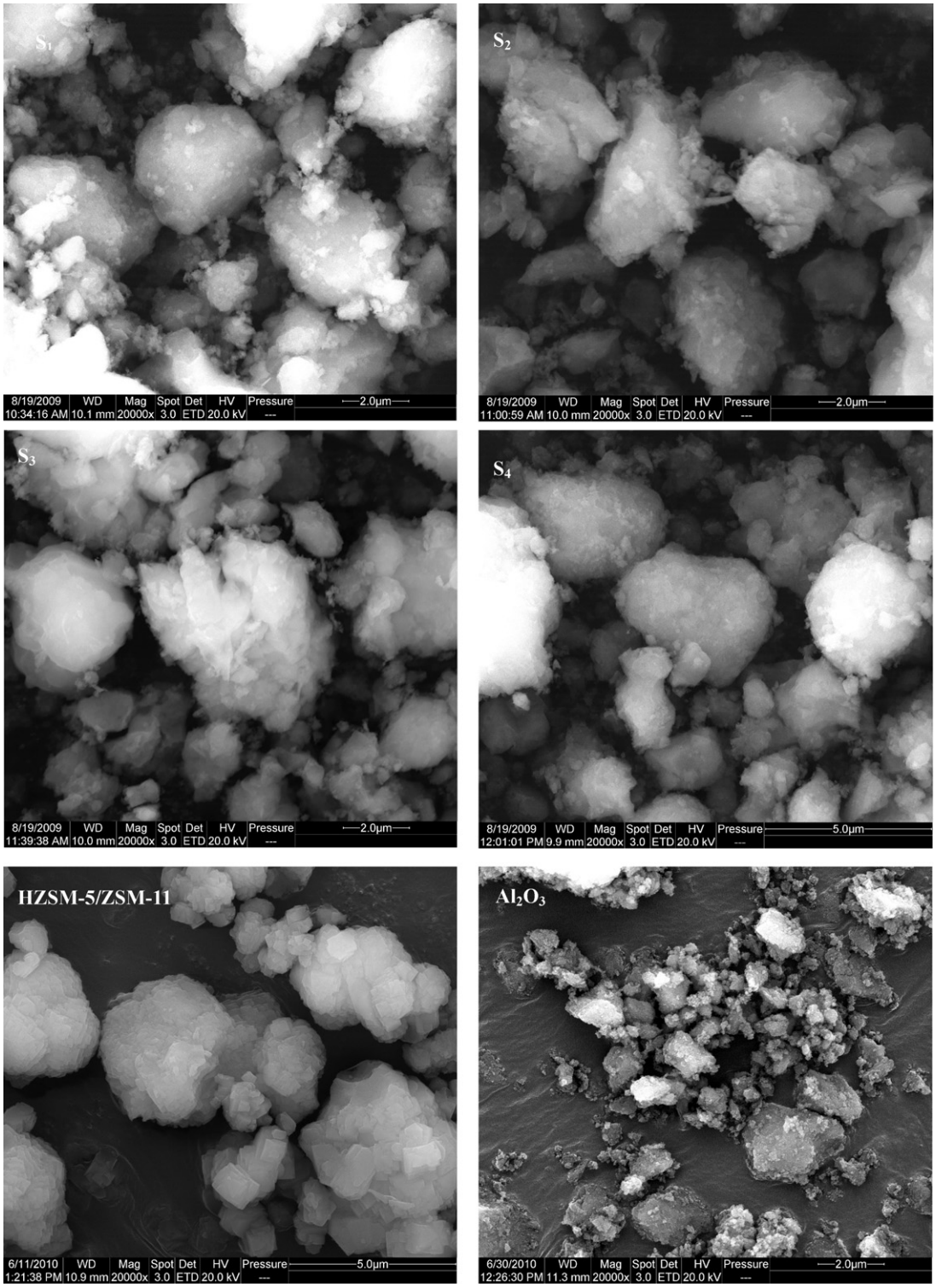

Fig. 2. SEM images of HZSM-5/ZSM-11-Al_2O_3 samples with different alkaline treatment conditions.

of alumina changed during the treatment process which could be further evidenced in following characterization results.

S_3 was obtained from ZSM-5/ZSM-11 zeolite without templates treated in NaOH solution before extrusion. Compared with S_1, S_3 showed an obvious increase in *l* peak intensity. This was in agreement with the previous reports about acidity changes in zeolite samples [17,18].

S_4 was obtained from ZSM-5/ZSM-11 zeolite containing templates treated in NaOH solution before extrusion. The total NH_3 desorption peak area was the biggest among four samples. Compared with S_1, not only *l* peak but also *h* peak intensity increased from 380 to 398 μmol/g indicating templates played an important role in keeping zeolites structure and acidity. Few reports could be found concerning the alkaline treatment for zeolites containing organic templates, especially for acidity changes [8,28,29]. Groen et al. pointed out that beta zeolite with template was inert to NaOH leaching and template-containing regions were protected from the silicon extraction [8]. However, this was not the case for ZSM-

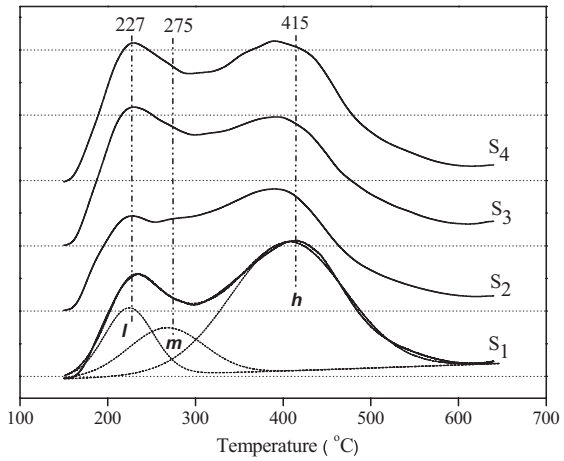

Fig. 3. NH_3-TPD profiles of HZSM-5/ZSM-11-Al_2O_3 samples with different alkaline treatment conditions.

5/ZSM-11 zeolite. Relative amount of weak and medium acid sites appeared after alkaline treatment without loss of strong acid sites after alkaline treatment.

3.2.2. Py-IR spectra

In order to get more information about the changes of Brϕnsted and Lewis acid sites, Py-IR spectra were carried out to determine the Brϕnsted/Lewis ratio of the samples. Fig. 4 shows the infrared spectra of adsorbed pyridine on different samples. The characteristic infrared bands near 1540 cm^{-1} are attributed to pyridine ions on Brϕnsted acid sites and those near 1450 cm^{-1} are corresponding to pyridine bonded to Lewis acid centers. As shown in Fig. 4, both Brϕnsted and Lewis acid sites were found on all samples. For S_2, the amount of Lewis acid sites was reduced compared with other samples. It could be deduced that Lewis acid sites were preferentially consumed during the alkaline treatment process for zeolite extrudate which was different from the case of pure ZSM-5 zeolite [16]. As alumina was the main source of Lewis acid sites, one question appeared whether the state of alumina had changed during the alkaline treatment process. One possible explanation was that part of the alumina binder in S_2 dissolved in the alkali-solution. This was also evidenced by the XRF elemental analysis results. For S_1, the original Si/Al ratio was 2.37. And the value increased to 2.50 in S_2 which was contrast to the case of the pure zeolite sample. Thus, it could be deduced that not only silicon in zeolites but also part of alumina binder was dissolved in the NaOH solution. However, no acidity distribution change could be observed over pure alumina sample before and after alkaline treatment as shown in Fig S1. For S_1, the B/L ratio was 0.99 and it increased to 2.3 for S_2. Little difference in B/L ratio was found between S_3 and S_4, as shown in Table 1. When the evacuation temperature increased to 300 °C, the peak intensity at 1450 cm^{-1} decreased indicating that acidity strength of Lewis acid sites was weaker than that of Brϕnsted acid sites. As listed in Table 1, the B/L ratio of all samples increased upon desorption temperature among which S_2 was the highest.

Combined with NH_3-TPD and Py-IR results, it could be deduced that alkaline treatment may change both the amount and distribution of acid sites. For S_2, due to the simultaneous removal of silicon in ZSM-5/ZSM-11 and alumina binder during alkaline treatment procedure, the number of weak and strong acid site was reduced. Meanwhile, the ratio of Lewis acid sites decreased. As to S_3, NaOH solution treatment led to the increase of acid sites at low desorption temperature. For S_4, total acidity increased especially for medium acid sites. The existence of organic template may protect the Si extraction in alkali-solution to some extent which prevented the zeolite framework from collapsing and the loss of acidity amount [8].

3.3. Texture and mass transfer properties

3.3.1. N_2 adsorption measurements

Alkaline treatment not only changed the samples' acidity distribution but also had influences on the pore structure of the samples. N_2 adsorption experiments were applied to get the information about surface area and pore distribution. As shown in Fig. 5, the N_2 adsorption–desorption isotherms for all samples showed a hysteresis loop ranging from $P/P_0 = 0.4$ to $P/P_0 = 1$. Existence of alumina binder accounted for the hysteresis loop in a micropore ZSM-5/ZSM-11 zeolite. It could be observed that the loop was relatively small for S_1 but much larger for S_2, which revealed that alkaline treatment process led to the creation of many mesopores. At the same time, the N_2 uptake amount of S_2 sample was higher than that of S_1. This could be further confirmed by the corresponding analysis results listed in Table 2. Samples after alkaline treatment possessed a little larger surface area compared with S_1. Meanwhile, S_2 had the largest mesopore volume up to 0.1534 cm^3/g. For S_3 and S_4, the mesopore number exhibited decreasing trend. From this point of view, alumina may contribute to the mesopore number during the alkaline treatment process. To verify this supposition, pure alumina sample was prepared and further treated with alkali-solution under the same conditions. As shown in Table S1, the total pore volume of pure alumina increased from 0.4937 to 0.5026 cm^3/g after alkaline treatment. However, the BET surface area of alumina decreased from 225.0 to 200.4 m^2/g after the alkaline treatment. This meant the pore structure of alumina binder in S_2 may change during the alkaline treatment process. However, the main contri-

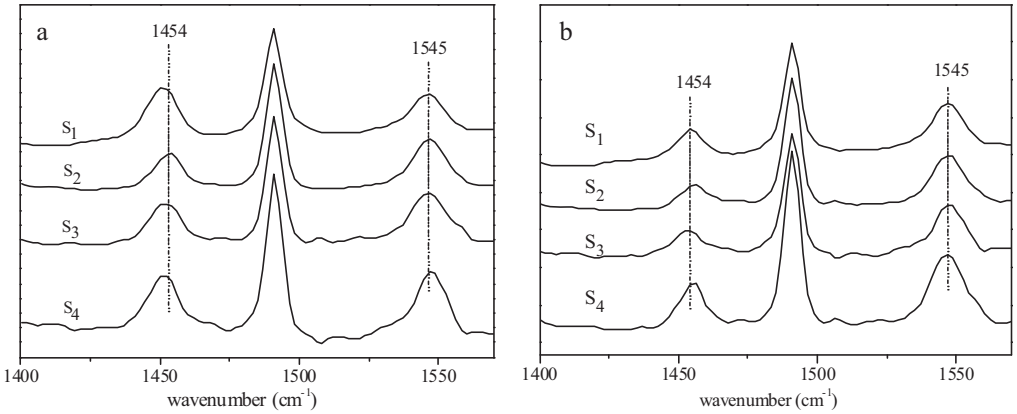

Fig. 4. Py-IR spectra of HZSM-5/ZSM-11-Al_2O_3 samples with different alkaline treatment conditions. (a) Evacuated at 150 °C for 0.5 h and (b) evacuated at 300 °C for 0.5 h.

Table 2
Textural properties of samples with different alkali-treatment conditions.

Sample	BET surface (m^2/g)	Micropore area (m^2/g)	External area (m^2/g)	Micropore volume (cm^3/g)	Mesopore volume (cm^3/g)
S_1	302.5	192.2	110.3	0.0944	0.1198
S_2	311.4	152.9	158.5	0.0752	0.1534
S_3	314.2	157.5	156.7	0.0775	0.1525
S_4	310.1	166.5	143.6	0.0820	0.1517

bution of mesopore amount in S_2 came from alkali-ZSM-5/ZSM-11 zeolite. Compared with S_4, the N_2 uptake amount of S_3 sample was a little higher. The existence of organic template in S_4 may restrain the silica extraction and the generation of mesopore. It should be pointed out that relative number of mesopore was still generated in S_4 compared with S_1.

3.3.2. Uptake profiles of cyclo-hexane and m-xylene using TEOM

Pore structure of samples may greatly affect the adsorption behavior of reactants and the diffusion of product molecules. To verify the special role of mesopore in mass transportation process, S_1 and S_2 were selected for the probe molecule uptake experiments, because they have the smallest and largest mesopore volumes of the four samples. *Cyclo*-hexane and *m*-xylene were chosen as the probe molecules to detect the adsorption behavior on different samples since their molecular size was similar to the molecular size of aromatic product in the 1-hexene aromatization reaction. TEOM, which showed high sensitivity, mass resolution and enabled real-time measurement, was applied to detect the mass changes during the adsorption process [30–32]. Compared with the traditional thermo gravimetric analysis instruments, the major advantage of TEOM was that it could better simulate the environment of real fixed bed reactor since all the gas was forced to flow through the catalyst bed. The structure enabled non-contact measurement of the mass change under real catalytic conditions and quick response to catalyst mass changes, which could give more real information about the mass transfer process.

As shown in Fig. 6a, the uptake rate of *cyclo*-hexane was extremely quick over S_1 and S_2. Only 0.35 s was required to reach 50% of the maximum uptake suggesting the small size molecule of *cyclo*-hexane could enter micropores very quickly. It could be deduced that in the aromatization reaction, the diffusion and desorption of *cyclo*-hexane molecule (or similar size molecule) was not the critical factor among all the products. While in the case of *m*-xylene, the situation was quite different (Fig. 6b). The dynamic diameter of *m*-xylene (6.8 Å) was a little larger than that of *cyclo*-hexane (6.0 Å). It was difficult for *m*-xylene molecule to diffuse in and out of the channel of ZSM-5/ZSM-11 zeolite. During the first 20 min, the uptake rate of *m*-xylene in S_2 was greatly enhanced, especially in the initial stage where the uptake rate was sharply increased and an uptake of 50% was achieved only after 2 min. After the equilibrium, no obvious change in adsorption amount for S_1 and S_2 was observed. The quick diffusion rate in S_2 was attributed to the mesopores created by alkaline treatment, as have been evidenced by the N_2 adsorption results. Due to the existence of alumina binder, it was difficult to choose a model to describe the diffusivity of the sample. In general, we could observe the enhanced mass transfer ability in S_2 especially for larger molecule such as *m*-xylene. This provided clear and direct evidences for the contribution of mesopore in molecule diffusion in aromatization reaction.

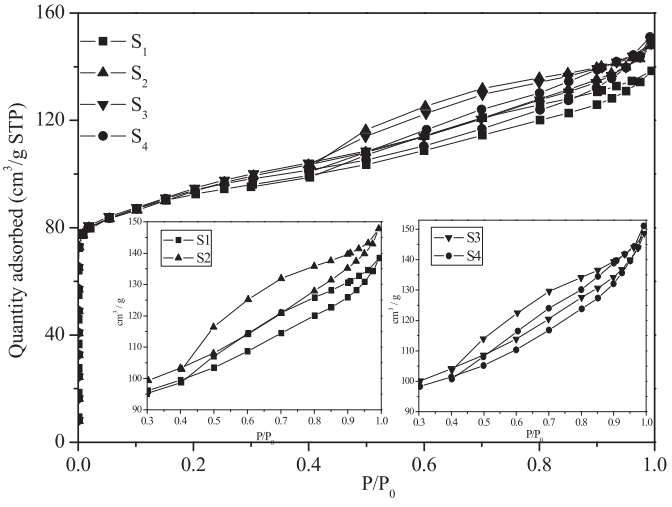

Fig. 5. N_2 adsorption isotherms of HZSM-5/ZSM-11-Al_2O_3 samples with different alkaline treatment conditions.

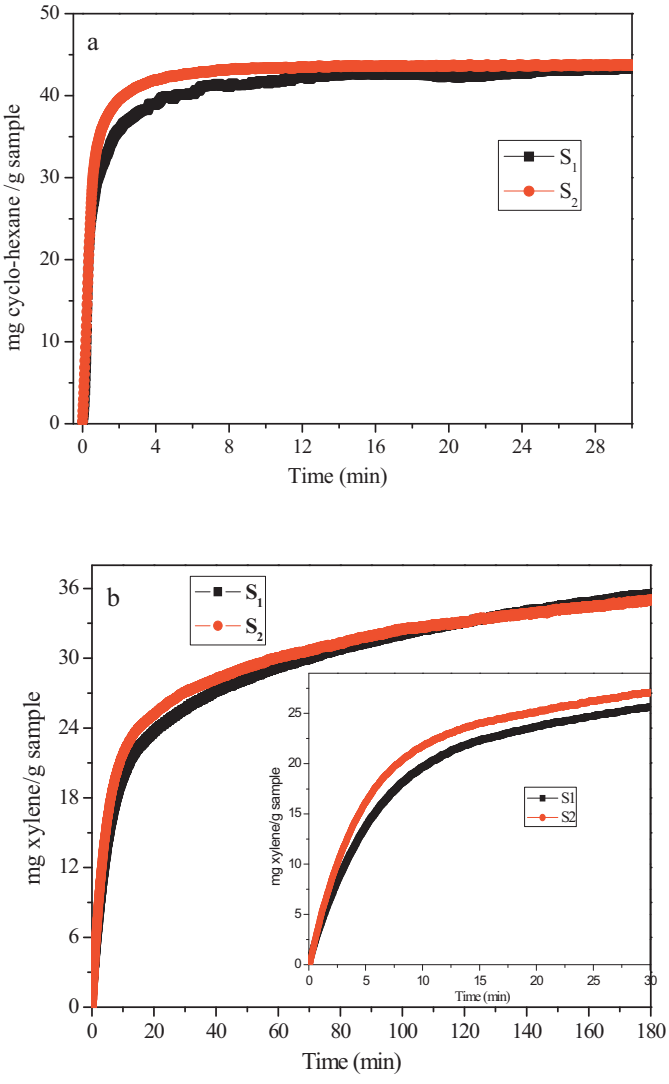

Fig. 6. (a) *Cyclo*-hexane uptake curves of S_1 and S_2 measured in the TEOM at 120 °C and (b) *m*-xylene uptake curves of S_1 and S_2 measured in the TEOM at 150 °C.

Table 3
1-Hexene transformation activity over HZSM-5/ZSM-11-Al_2O_3 catalysts (using alumina as binder) with different alkali-treatment conditions.

	S_1		S_2		S_3		S_4	
	1–4 h	5–8 h	1–4 h	5–8 h	1–4 h	5–8 h	1–4 h	5–8 h
Fuel gas (wt.%)	0.3	0.2	0.2	0.2	0.2	0.2	0.2	0.2
LPG (wt.%)	21.5	20.7	21.5	20.0	21.6	20.3	21.6	20.5
Liquid product (wt.%)	78.2	79.1	78.3	79.8	78.2	79.5	78.2	79.3
Liquid product distribution (wt.%)								
n-Paraffin	8.0	10.2	7.8	8.5	8.2	9.3	8.0	10.2
i-Paraffin	28.4	32.3	28.2	29.7	29.3	30.7	28.0	34.1
Olefin	5.0	13.9	5.5	6.4	5.5	14.3	4.0	13.2
Naphthene	4.0	4.8	4.9	5.1	4.3	4.9	4.3	5.0
Aromatics	54.6	38.8	53.6	50.3	52.7	40.8	55.7	37.5

3.4. Catalytic performances in 1-hexene isomerization and aromatization reaction

Previous study of our group demonstrated that the reaction stability of butene and 1-hexene aromatization could be dramatically improved over the alkali-treated pure HZSM-5 zeolite [14–16]. Here, 1-hexene transformation was applied as probe reaction to investigate the influences of alkaline treatment sequence on catalytic activities of HZSM-5/ZSM-11 zeolites with alumina as binder. Detailed evaluation data and product distributions were listed in Table 3. The liquid yield was around at 78% during the first 4 h. With longer time on stream, the yield increased a little due to the loss of acid sites upon reaction. No obvious difference was found among the four samples for *iso*-paraffin selectivity, indicating that the *iso*-paraffin distribution was not affected by the alkaline treatment. However, this was not the same case for aromatics distribution. For S_1 which was prepared by ZSM-5/ZSM-11 zeolite extruded with alumina, the aromatics content in the liquid was up to 54.6% during the first 4 h and it dropped to 38.8% with 8 h on stream. After alkaline treatment with S_1, S_2 showed better catalytic stability and its aromatics content changed from 53.6% during the first 4 h to 50.3% upon reaction time. The existence of mesopores, which was evidenced by N_2 adsorption and *m*-xylene adsorption measurements, played an important role for the better catalytic stability. Previous studies revealed that the number of acidity and mesopore both greatly influenced the 1-hexene isomerization and aromatization activity [14]. For pure ZSM-5 zeolite, moderate alkaline treatment could increase the amount of weak acid sites and mesopores. In this case, the alkaline treatment after sample extrusion with binder not only decreased the weak acid sites amount but also changed the acidity distribution in S_2. This meant that alumina binder also participated in the process. The removal of weak acid sites from Al_2O_3 may contribute to the better catalytic performance of S_2. Although there also existed relative amount of mesopores in S_3, its catalytic activity declined quickly. This may be related with the large number of weak acid sites and a balance between Brϕnsted and Lewis acid sites was needed to guarantee the good aromatization activity [33]. For S_4, its initial aromatization activity was comparable to that of S_2. However, poor catalytic stability and aromatics content loss was observed over S_4 which was attributed to the less number of mesopore. In other words, the existence of organic template in ZSM-5/ZSM-11 prohibited the formation of mesopore during alkali-treatment process.

On basis of the discussion above, alkaline treatment sequences not only changed the acidity amount and distribution of ZSM-5/ZSM-11-Al_2O_3 samples but also altered the number of introduced mesopores. S_2 sample prepared with alkaline treatment after extrusion showed best performance in the 1-hexene isomerization and aromatization reaction. Suitable medium and strong acid sites ratio in S_2 modified by NaOH solution contributed to the high aromatization activity. The existence of largest amount of mesopore facilitated the quick diffusion of product molecule, especially for xylene which improved the reaction stability. Meanwhile, our results suggested that part of the alumina binder dissolved in the alkaline solution during the treatment process and textural properties of alumina also changed. Alkaline treatment to ZSM-5/ZSM-11 zeolite containing organic template may increase the total acid amount as verified in S_4. During the treatment process, the existence of template limited the Si extraction from zeolite framework and only small number of mesopore was generated compared with that of no organic templates. Further studies about the role of template in alkaline treatment process are in progress. The enhancement of acidity and mesopore amount in S_4 may be good for other catalytic applications.

4. Conclusion

Four ZSM-5/ZSM-11-Al_2O_3 samples with different alkali-treatment sequences were prepared and evaluated by the 1-hexene isomerization and aromatization reaction. As revealed by NH_3-TPD and Py-IR results, alkaline modification at different preparation step may lead to different changes of acidity amount and distribution. The best treatment way for ZSM-5/ZSM-11 sample using alumina as binder in the aromatization reaction was found as zeolites extrusion with successive alkaline treatment as shown in S_2. Silicon extraction of zeolites and aluminum loss from binder happened simultaneously during the alkaline treatment process. Acidity redistribution and the introduction of new mesopores were proved to play an important role for the improved aromatization activity and reaction stability. Better mass transfer performance for aromatic molecules in S_2 was further verified by the *m*-xylene up-take experiments using TEOM.

Acknowledgments

We are grateful for the financial support of the National Natural Science Foundation of China (grant nos. 20903088 and 20773120) and the Ministry of Science and Technology of China through the National Key Project of Fundamental Research (grant no. 2009CB623507). We thank Prof. Xinhe Bao and Dr. Xiulian Pan of Dalian Institute of Chemical Physics, CAS for the help with TEOM measurements.

Appendix A. Supplementary data

Supplementary data associated with this article can be found, in the online version, at doi:10.1016/j.molcata.2010.12.007.

References

[1] Y. Tao, H. Kanoh, L. Abrams, K. Kaneko, Chem. Rev. 106 (2006) 896–910.
[2] S.T. Tsai, C.H. Chen, T.C. Tsai, Green Chem. 11 (2009) 1349–1356.
[3] X.F. Li, R. Prins, J.A. van Bokhoven, J. Catal. 262 (2009) 257–265.
[4] M. Choi, K. Na, J. Kim, Y. Sakamoto, O. Terasaki, R. Ryoo, Nature 461 (2009), 246-U120.

[5] W. Fan, M.A. Snyder, S. Kumar, P.S. Lee, W.C. Yoo, A.V. McCormick, R.L. Penn, A. Stein, M. Tsapatsis, Nat. Mater. 7 (2008) 984–991.
[6] J.C. Groen, T. Bach, U. Ziese, A.M. Paulaime-van Donk, K.P. de Jong, J.A. Moulijn, J. Perez-Ramirez, J. Am. Chem. Soc. 127 (2005) 10792–10793.
[7] M. Ogura, S. Shinomiya, J. Tateno, Y. Nara, M. Nomura, E. Kikuchi, M. Matsukata, Appl. Catal. A: Gen. 219 (2001) 33–43.
[8] J. Perez-Ramirez, S. Abello, A. Bonilla, J.C. Groen, Adv. Funct. Mater. 19 (2009) 164–172.
[9] J.C. Groen, J.A. Moulijn, J. Perez-Ramirez, J. Mater. Chem. 16 (2006) 2121–2131.
[10] J. Perez-Ramirez, C.H. Christensen, K. Egeblad, J.C. Groen, Chem. Soc. Rev. 37 (2008) 2530–2542.
[11] F. Jin, Y. Cui, Y. Li, Appl. Catal. A: Gen. 350 (2008) 71–78.
[12] S. Gopalakrishnan, A. Zampieri, W. Schwieger, J. Catal. 260 (2008) 193–197.
[13] J.C. Groen, S. Abello, L.A. Villaescusa, J. Perez-Ramirez, Micropor. Mesopor. Mater. 114 (2008) 93–102.
[14] Y.N. Li, S.L. Liu, Z.K. Zhang, S.J. Xie, X.X. Zhu, L.Y. Xu, Appl. Catal. A: Gen. 338 (2008) 100–113.
[15] Y.N. Li, S.L. Liu, S.J. Xie, L.Y. Xu, Appl. Catal. A: Gen. 360 (2009) 8–16.
[16] Y. Song, X. Zhu, Y. Song, Q. Wang, L. Xu, Appl. Catal. A: Gen. 302 (2006) 69–77.
[17] J.C. Groen, J.C. Jansen, J.A. Moulijn, J. Perez-Ramirez, J. Phys. Chem. B 108 (2004) 13062–13065.
[18] J.C. Groen, L.A.A. Peffer, J.A. Moulijn, J. Perez-Ramirez, Chem. Eur. J. 11 (2005) 4983–4994.
[19] J.C. Groen, J.A. Moulijn, J. Perez-Ramirez, Micropor. Mesopor. Mater. 87 (2005) 153–161.
[20] W.H. Chen, S.J. Huang, C.S. Lai, T.C. Tsai, H.K. Lee, S.B. Liu, Res. Chem. Intermed. 29 (2003) 761–772.
[21] J.C. Groen, J.A. Moulijn, J. Perez-Ramirez, Ind. Eng. Chem. Res. 46 (2007) 4193–4201.
[22] Q.X. Wang, S.R. Zhang, G.Y. Cai, F. Li, L.Y. Xu, Z.X. Huang, Y.Y. Li, Alkylation catalyst of zeolite and porous inorganic oxide gives high selectivity and conversion rate for the production of ethylbenzene, WO9749489-A, China Petro. Chem. Corp, Dalian Inst. Chem. Phys. CAS, Fushun Petro. Chem. Co. Sinopec, 1997.
[23] L.Y. Xu, J.X. Liu, Q.X. Wang, S.L. Liu, W.J. Xin, Y.D. Xu, Appl. Catal. A: Gen. 258 (2004) 47–53.
[24] L. Zhang, H.J. Liu, X.J. Li, S.J. Xie, Y.Z. Wang, W.J. Xin, S.L. Liu, L.Y. Xu, Fuel Process. Technol. 91 (2010) 449–455.
[25] Q.X. Wang, S.R. Zhang, G.Y. Cai, F. Li, L.Y. Xu, Z.X. Huang, Y.Y. Li, Rare earth-ZSM-5/ZSM-11 cocrystalline zeolites, CN94113403, China Petro. Chem. Corp, Dalian Inst. Chem. Phys. CAS, Fushun Petro. Chem. Co. Sinopec, 1994.
[26] C.A. Emeis, J. Catal. 141 (1993) 347–354.
[27] K. Foger, J.V. Sanders, D. Seddon, Zeolites 4 (1984) 337–345.
[28] A. Imek, B. Suboti, I. Mit, A. Tonejc, R. Aiello, F. Crea, A. Nastro, Micropor. Mater. 8 (1997) 159–169.
[29] X. Wei, P.G. Smirniotis, Micropor. Mesopor. Mater. 97 (2006) 97–106.
[30] J.C. Groen, W.D. Zhu, S. Brouwer, S.J. Huynink, F. Kapteijn, J.A. Moulijn, J. Perez-Ramirez, J. Am. Chem. Soc. 129 (2007) 355–360.
[31] W.D. Zhu, J.M. van de Graaf, L.J.P. van den Broeke, F. Kapteijn, J.A. Moulijn, Ind. Eng. Chem. Res. 37 (1998) 1934–1942.
[32] W.D. Zhu, J.C. Groen, F. Kapteijn, J.A. Moulijn, Langmuir 20 (2004) 5277–5284.
[33] P.Q. Zhang, X.W. Guo, H.C. Guo, X.S. Wang, J. Mol. Catal. A: Chem. 261 (2007) 139–146.